

# Explanation of observed features of self-organization in traffic flow

Martin Treiber and Dirk Helbing

*II. Institute of Theoretical Physics, University of Stuttgart, Pfaffenwaldring 57/III, D-70550 Stuttgart, Germany*  
(February 1, 2008)

Based on simulations with the “intelligent driver model”, a microscopic traffic model, we explain the recently discovered transition from free over “synchronized” traffic to stop-and-go patterns [B. S. Kerner, *Phys. Rev. Lett.* **81**, 3797 (1998)]. We obtain a nearly quantitative agreement with empirical findings such as the “pinch effect”, the flow-density diagram, the emergence of stop-and-go waves from nonhomogeneous congested traffic, and the dimensions of their wavelength.

05.70.Fh, 05.65.+b, 47.54.+r, 89.40.+k

During the last years, theoretical and empirical investigations have identified different possible mechanisms for a phase transition from free traffic to stop-and-go traffic on freeways. This includes deterministic [1–4] and stochastic mechanisms [5–8] as well as effects of inhomogeneities [9–12]. In contrast, Kerner has recently described the detailed features of another transition to stop-and-go patterns [13] developing from “synchronized” congested traffic [14,15] on German highways, which are compatible with empirical findings on Dutch highways [16].

In the following, we propose a quantitative explanation of these observations based on microsimulations with the “intelligent driver model” (IDM). In particular, we will show the possible coexistence of different traffic states along the road behind an inhomogeneity of traffic flow. It is, in upstream direction, associated with the sequence “homogeneous congested traffic” [10,11] (which, in a multilane model, is related to the observed synchronization among lanes [9,17]) → “inhomogeneous congested traffic” [11] (corresponding to the so-called “pinch region” [13]) → “stop-and-go traffic”, while we have free traffic flow downstream of the inhomogeneity.

It will turn out that, in contrast to previously reported traffic phenomena, this phenomenon relies on the existence of a sufficiently large density region of convectively stable traffic, in which traffic flow is unstable, but any perturbations are convected away in upstream direction. Furthermore, one needs a traffic model in which the resulting traffic flow inside of fully developed traffic jams is much lower (nearly zero) than in “synchronized” traffic. In particular, without suitable modifications (see below), this is not satisfied by the traffic model discussed in Ref. [10]. We also point out that, although the IDM has a unique flow-density relation in equilibrium, it reproduces the observed two-dimensional scattering of flow-density data at medium vehicle densities [14,13], even without assuming a mixture of different vehicle types [18].

The IDM is a continuous, deterministic model, in which the acceleration of a vehicle  $\alpha$  of length  $l_\alpha$  at position  $x_\alpha(t)$  depends on its own velocity  $v_\alpha(t)$  as well as

the gap  $s_\alpha(t) = [x_{\alpha-1}(t) - x_\alpha(t) - l_\alpha]$  and the velocity difference  $\Delta v_\alpha(t) = [v_\alpha(t) - v_{\alpha-1}(t)]$  to the vehicle  $(\alpha-1)$  in front:

$$\dot{v}_\alpha = a \left[ 1 - \left( \frac{v_\alpha}{v_0} \right)^\delta - \left( \frac{s^*}{s_\alpha} \right)^2 \right]. \quad (1)$$

According to this formula, the acceleration on a free road (meaning  $s_\alpha \rightarrow \infty$ ) is given by  $a[1 - (v_\alpha/v_0)^\delta]$ , where  $a$  is the maximum acceleration and  $v_0$  the desired velocity. The exponent  $\delta$  is typically between 1 and 5. It allows to describe that the realistic acceleration behavior of drivers lies between a constant acceleration  $a$  up to their desired velocity  $v_0$  ( $\delta \rightarrow \infty$ ) and an exponential acceleration behavior ( $\delta = 1$ ).

The braking term  $-a(s^*/s_\alpha)^2$  depends Coulomb-like on the gap  $s_\alpha$ , as it is the case for the braking term of the microscopic Wiedemann model [19]. Therefore, the acceleration term is negligible, if the gap  $s_\alpha$  drops considerably below the “effective desired distance”  $s^*$ . With the relation

$$s^*(v_\alpha, \Delta v_\alpha) = s_0 + \max \left( v_\alpha T + \frac{v_\alpha \Delta v_\alpha}{2\sqrt{ab}}, 0 \right), \quad (2)$$

it is constructed in a way that drivers keep a minimum “jam distance”  $s_0$  to a standing vehicle, plus an additional safety distance  $v_\alpha T$ , where  $T$  is the safe time headway in congested but moving traffic.

The nonequilibrium term proportional to  $\Delta v_\alpha$  [2,8] reflects an “intelligent” braking strategy, according to which drivers restrict their deceleration to  $b$  in “normal” situations (e.g., when approaching standing or slower vehicles from sufficiently large distances), but they brake harder when the situation becomes more critical, i.e., when the anticipated “kinematic deceleration”  $(\Delta v)^2/(2s_\alpha)$ , which is necessary to avoid a collision with a uniformly moving leading vehicle ( $\dot{v}_{\alpha-1} = 0$ ), exceeds  $b$ . Notice that the acceleration  $a$  is typically lower than the desired deceleration  $b$ , and that both acceleration parameters do not influence the equilibrium flow-density relation (“fundamental diagram”). Since it turns out that

neither multilane effects nor different types of vehicles are relevant in the context of this study, we have assumed identical “driver-vehicle units” characterized by the realistic parameters  $v_0 = 120$  km/h,  $\delta = 4$ ,  $a = 0.6$  m/s<sup>2</sup>,  $b = 0.9$  m/s<sup>2</sup>,  $s_0 = 2$  m, and  $T = 1.5$  s, apart from a localized change of  $v_0$  or  $T$  (see below). For the vehicle length we use  $l = 5$  m, but this value does not affect the dynamics.

We simulated an open freeway section of 20 kilometer length for time intervals up to 120 minutes, of which we display the most interesting parts only. In addition, we assumed an inhomogeneity of traffic flow that will be responsible for the transition from free to congested traffic, as described in Refs. [10,11]. However, as pointed out by Kerner [13], the self-organized patterns observed by him are not restricted to the vicinity of on-ramps. We will confirm this by simulating different kinds of inhomogeneities (see Figs. 1 through 3) and comparing them with the injection of vehicles at on-ramps (see Fig. 4).

In Figure 1, we have assumed an inhomogeneity corresponding to a freeway section where people drive more carefully. This was modelled by setting the desired time headway from  $T = 1.5$  s to  $T = 1.75$  s between  $x = 0$  km and  $x = 0.3$  km. In the simulations of Figs. 2 and 3, we have reduced the desired velocity from  $v_0 = 120$  km/h to  $v_0 = 80$  km/h in the same region. As initial conditions, we assumed homogeneous free traffic in equilibrium at a flow of  $Q_0 = 1670$  vehicles/h (Figs. 1 through 3) or 1570 vehicles/h (Fig. 4). The actual initial conditions, however, are only relevant for a short time interval. At the upstream boundary, we assume that vehicles enter the freeway uniformly at a rate  $Q_{\text{in}}(t) = Q_0 + \Delta Q(t)$  and drive with a velocity corresponding to free traffic in equilibrium. While in the simulation of Fig. 1, the breakdown of traffic flow is caused by exceeding the static freeway capacity at the inhomogeneity [11], in Figs. 2 and 3 it is triggered by a triangularly shaped perturbation  $\Delta Q(t)$  of the inflow [10,11] between  $t = 10$  min and  $t = 20$  min with a maximum of 200 vehicles per hour and lane at  $t = 15$  min. Furthermore, we used the “absorbing” downstream boundary condition  $\dot{v}_\alpha = 0$ . To minimize simulation time, we integrated Eq. (1) with a simple Euler scheme using a coarse time discretization of  $\Delta t = 0.4$  s, and translated the vehicles in each step according to  $x_\alpha(t + \Delta t) = x_\alpha(t) + v_\alpha \Delta t + \frac{1}{2} \dot{v}_\alpha (\Delta t)^2$ . However, smaller values of  $\Delta t$  yielded nearly indistinguishable results.

Figure 1 gives a representative overview of the simulation result by means of a spatiotemporal density plot. The resulting sequence of transitions is essentially the same as observed [13]: After 10 minutes of free traffic, traffic breaks down near the inhomogeneity, resulting in homogeneous congested traffic at this location, that persists over a long time. Upstream of the inhomogeneity, small oscillations develop that travel further upstream and grow to stop-and-go waves of relatively short wavelengths (about 0.8 km). Finally, these waves either dis-

solve or merge to a few “wide jams” (in which traffic comes to a standstill) with typical distances of 2 km up to 5 km between them. Once the jams have formed, they persist and propagate upstream at a constant propagation velocity without further changes of their shape. No new clusters develop between the jams.

To compare our simulation results directly with the empirical data published by Kerner [13], we investigated the temporal evolution of the average velocity at six subsequent locations D1 through D6 that had the same distances with respect to the inhomogeneity as in Ref. [13] (see Fig. 2). The detector positions D1 through D4 are upstream of the inhomogeneity, D5 is directly at the inhomogeneity, and D6 is downstream of it. In contrast to the simulation of Fig. 1, the capacity drop at the inhomogeneity is so weak that free traffic is metastable in the overall system. At the inhomogeneity (D5), one observes homogeneous congested (“synchronized”) traffic, at D4 one sees small oscillations that, around D3, develop to stop-and-go waves of larger amplitude, and finally to jams (at D1 and D2). In the downstream direction, the congested traffic dissolves to free traffic (D6). Apart from irregularities in the measured data due to fluctuations, the curves are in (semi-)quantitative agreement with Kerner’s empirical findings [13].

We also plot one-minute data of the six “detectors” in a flow-density diagram (Fig. 3), together with the equilibrium flow-density relation  $Q_e(\rho)$  (“fundamental diagram”). The lower boundary of the data points at medium densities corresponds to the flow-density relation belonging to the downstream front of a fully developed jam. In agreement with observations, this line is the same for all jams and corresponds to a unique propagation velocity of their downstream fronts. The twodimensional region of points above this line relate to congested traffic at D3, D4, and D5.

To understand this scenario, we need some basic results about the stability of homogeneous traffic with respect to localized perturbations. Typically, there are four “critical” densities  $\rho_{ci}$  with  $\rho_{c1} < \rho_{c2} < \rho_{c3} < \rho_{c4}$  and the following properties [20,21]: For low and very high densities ( $\rho < \rho_{c1}$  or  $\rho > \rho_{c4}$ ), traffic is stable with respect to arbitrary perturbations, while for  $\rho_{c2} < \rho < \rho_{c3}$ , it is linearly unstable. In the two density ranges in between, homogeneous traffic is unstable only with respect to perturbations exceeding a certain critical amplitude  $\Delta \rho_{cr}(\rho)$  (“metastability”). Furthermore, there exists a range  $\rho_{cv} < \rho < \rho_{c3}$  with  $\rho_{cv} > \rho_{c2}$ , where traffic is linearly unstable, but convectively stable, i.e., all perturbations grow, but they are eventually convected away in upstream direction [22]. Actually, this range can be very large. For the IDM with the parameters used here, we have  $\rho_{cv} = 50$  vehicles/km and  $\rho_{c3} = 100$  vehicles/km.

Let us assume that the inflow  $Q_{\text{in}}$  has a value larger than  $Q_{c1}$ , and that a phase transition from free to congested traffic has occurred at the inhomogeneity. This

breakdown to congested traffic, which we identify with “synchronized traffic”, here [10,11,17,18], was explained in [10]. Since it is connected with a drop of the *effective* freeway capacity to the self-organized outflow  $\tilde{Q}_{\text{out}}$  from “synchronized” traffic (ST), the region of congested traffic will grow in upstream direction until the inflow  $Q_{\text{in}}(t) = Q_e(\rho_{\text{in}}(t))$  to the freeway falls below the synchronized flow  $Q_{\text{ST}}$  in the congested region behind the inhomogeneity. Without an on-ramp flow  $Q_{\text{ramp}}$  per freeway lane, we have  $Q_{\text{ST}} = \tilde{Q}_{\text{out}}$ , otherwise it is  $Q_{\text{ST}} = (\tilde{Q}_{\text{out}} - Q_{\text{ramp}})$  [10]. In contrast to the empirical findings explained in Ref. [10], the synchronized flow must be so high, here, that it is linearly unstable, which implies  $Q_{\text{ST}} > Q_e(\rho_{\text{c}3})$ . Therefore, small perturbations will grow to larger oscillations, which propagate in upstream direction faster than the congested region grows. When the oscillations reach the metastable region of free traffic upstream of the inhomogeneity, oscillations with an amplitude below the critical amplitude  $\Delta\rho_{\text{cr}}(\rho_{\text{in}})$  will eventually disappear, the remaining ones will continue to grow until they are fully developed traffic jams. We point out that a sequence of such jams is sustained, because the propagation velocity  $v_g$  and the outflow  $Q_{\text{out}} \approx Q_e(\rho_{\text{c}1})$  from jams are characteristic constants [23,24]. Finally, if the inhomogeneity is such that the synchronized flow is convectively stable, i.e.,  $Q_{\text{ST}} < Q_{\text{cv}} = Q_e(\rho_{\text{cv}})$ , the perturbations cannot propagate downstream (in contrast to small perturbations in free traffic). Hence, the front of dissolving traffic is smooth, then, and a small region of homogeneous congested traffic forms near the inhomogeneity [Figs. 1, 2(a), and 4].

In Fig. 3, the flow-density relation of the downstream front of a fully developed jam (where the velocity is zero) corresponds to a straight line, the slope of which is  $v_g$  [23]. Notice that this line (which in Fig. 3 and in Ref. [13] is labelled by “J”) lies considerably below the equilibrium curve  $Q_e(\rho)$ . On the other hand, traffic flow in the region of oscillating congested traffic is nearly in equilibrium as long as the oscillations are small. As the oscillations grow, the data points gradually approach the line J. This explains the observed twodimensionality of the congested part of the flow-density diagram. We point out that mixtures of different types of driver-vehicle units lead to to further effects contributing to an even wider scattering of flow-density points in the congested regime [18].

In summary, we have shown that the emergence of stop-and-go waves out of synchronized traffic, their coexistence, and the twodimensional scattering of data in the congested part of the flow-density diagram can be explained in the framework of “standard” traffic models that have a unique equilibrium flow-density relation. The necessary conditions are a metastability of traffic flow, a flow inside of traffic jams that is much lower than in synchronized congested traffic, and a sufficiently large density regime of linearly unstable traffic flow that is con-

vectively stable. If “synchronized” traffic is linearly unstable and free traffic upstream is metastable, upstream-moving perturbations will grow and, when their amplitudes became large enough, eventually form stop-and-go waves. To maintain this mechanism, the region of synchronized traffic behind the inhomogeneity must persist (i.e. it must not dissolve to stop-and-go waves), which is only the case if it is convectively stable. The twodimensionality of the congested branch of the flow-density diagram originates from the fact that the nonhomogeneous congested states are not in equilibrium.

The phenomenon should be widespread since it is triggered at relatively small inhomogeneities whenever traffic flow  $Q_{\text{in}}(t)$  exceeds a certain threshold  $Q_{\text{c}1}$ . Note that it can be also simulated with other traffic models like the macroscopic gas-kinetic-based model [21], if “frustration effects” are additionally taken into account (see Fig. 4).

The authors are grateful for financial support by the BMBF (research project SANDY, grant No. 13N7092) and by the DFG (Heisenberg scholarship He 2789/1-1).

- 
- [1] B. S. Kerner and P. Konhäuser, Phys. Rev. E **50**, 54 (1994).
  - [2] D. Helbing, *Verkehrsdynamik* (Springer, Berlin, 1997).
  - [3] C. Wagner *et al.*, Phys. Rev. E **54**, 5073 (1996).
  - [4] M. Bando, K. Hasebe, A. Nakayama, and Y. Sugiyama, Phys. Rev. E **51**, 1035 (1995).
  - [5] K. Nagel and M. Schreckenberg, J. Phys. I (France) **2**, 2221 (1992).
  - [6] M. Schreckenberg, A. Schadschneider, K. Nagel, and N. Ito, Phys. Rev. E **51**, 2939 (1995).
  - [7] S. Krauss and P. Wagner, Phys. Rev. E **55**, 5597 (1997).
  - [8] D. E. Wolf, *Physica A*, in print (1999).
  - [9] H. Y. Lee, H. W. Lee, and D. Kim, Phys. Rev. Lett. **81**, 1130 (1998).
  - [10] D. Helbing and M. Treiber, Phys. Rev. Lett. **81**, 3042 (1998).
  - [11] D. Helbing, A. Hennecke, and M. Treiber, preprint cond-mat/9809324, submitted to Phys. Rev. Lett. (1998).
  - [12] D. Helbing and M. Treiber, Science **282**, 2001 (1998).
  - [13] B. S. Kerner, Phys. Rev. Lett. **81**, 3797 (1998).
  - [14] B. S. Kerner and H. Rehborn, Phys. Rev. E **53**, R4275 (1996).
  - [15] B. S. Kerner and H. Rehborn, Phys. Rev. Lett. **79**, 4030 (1997).
  - [16] D. Helbing, Phys. Rev. E **55**, R25 (1997).
  - [17] V. Shvetsov and D. Helbing, *Macroscopic dynamics of multi-lane traffic*, Phys. Rev. E, submitted (1998).
  - [18] M. Treiber and D. Helbing, J. Phys. A: Math. Gen. **32**, L17 (1999).
  - [19] R. Wiedemann, *Simulation des Straßenverkehrsflusses. "Schriftenreihe des IfV"*, Vol. 8 (Institut für Verkehrswesen, University of Karlsruhe, Germany, 1974).
  - [20] B. S. Kerner, P. Konhäuser, and M. Schilke, Phys. Lett.

A **215**, 45 (1996).

- [21] M. Treiber, A. Hennecke, and D. Helbing, Phys. Rev. E **59**, 239 (1999).
- [22] M. C. Cross and P. C. Hohenberg, Rev. Mod. Phys. **65**, 851 (1993).
- [23] B. S. Kerner and H. Rehborn, Phys. Rev. E **53**, R1297 (1996).
- [24] B. S. Kerner, S. L. Klenov, and P. Konhäuser, Phys. Rev. E **56**, 4200 (1997).

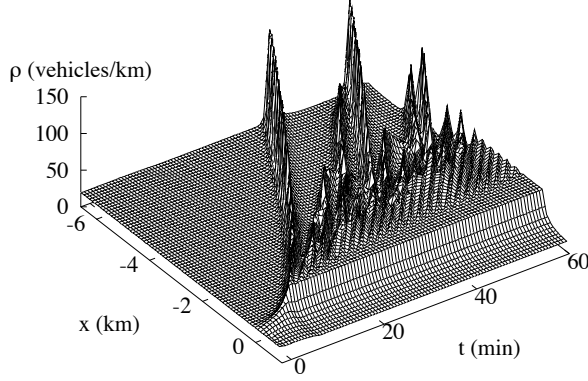


FIG. 1. Spatiotemporal density plot illustrating the breakdown to “synchronized” traffic (smooth region of high density) near an inhomogeneity, and showing stop-and-go waves emanating from this region. Traffic flows in positive  $x$ -direction. The inhomogeneity corresponds to an increased safe time headway  $T$  between  $x = 0$  km and  $x = 0.3$  km, reflecting more careful driving (see main text). Downstream of the inhomogeneity, vehicles accelerate into free traffic.

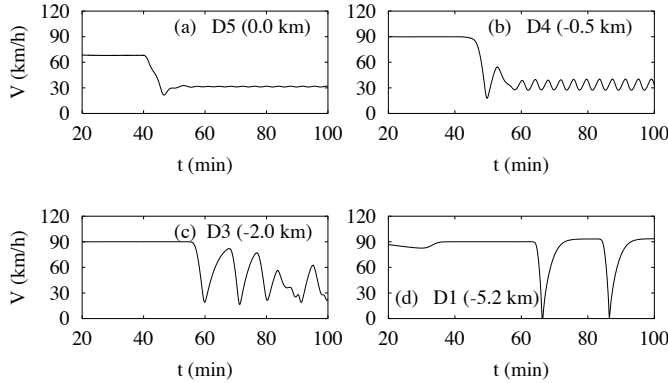


FIG. 2. Temporal evolution of the average velocity determined from the individual velocities of the vehicles that pass cross sections of the freeway during one-minute intervals at the four “detector” positions D1, D3, D4 (upstream of the inhomogeneity), and D5 (at the inhomogeneity). The naming of the detectors and their distances with respect to the inhomogeneity are the same as in Ref. [13]. The inhomogeneity is realized by a drop of the desired velocity (see the main text). (a) Breakdown to homogeneous synchronized traffic around  $t = 45$  min. (b) Oscillating synchronized traffic (“pinch region”), (c) developing stop-and-go waves, and (d) resulting traffic jams.

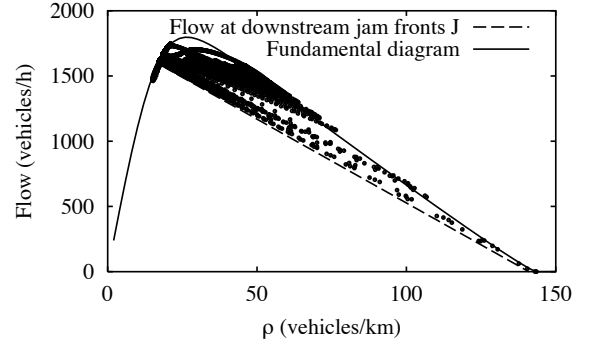


FIG. 3. Flow-density data (symbols) calculated from the microscopic simulation at the four detector locations displayed in Fig. 2, and in addition at  $x = -3.7$  km (detector D2) and at  $x = 1.2$  km (D6). Also shown is the equilibrium flow-density relation (solid line), and the flow-density relation at the downstream fronts of fully developed jams (dashed).

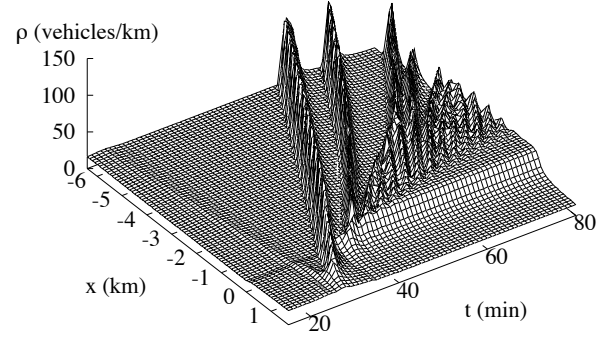


FIG. 4. Spatiotemporal evolution of the traffic density according to the gas-kinetic-based traffic model [21]. The assumed inhomogeneity of traffic flow comes from an on-ramp of length 200 m with an inflow of 220 vehicles per hour and freeway lane. The inflow to the main road is 1570 vehicles per hour and lane, and the breakdown of traffic flow is triggered by a perturbation  $\Delta Q(t)$  of the inflow with a flow peak of 125 vehicles per hour and lane (see main text). The assumed model parameters are  $V_0 = 120$  km/h,  $T = 1.5$  s,  $\tau = 30$  s,  $\rho_{\max} = 120$  vehicles/km, and  $\gamma = 1.2$ , while the parameters for the variance prefactor [21]  $A(\rho) = A_0 + \Delta A \{ \tanh[(\rho - \rho_c)/\Delta\rho] + 1 \}$  are  $A_0 = 0.008$ ,  $\Delta A = 0.02$ ,  $\rho_c = 0.27\rho_{\max}$ , and  $\Delta\rho = 0.1\rho_{\max}$ . In order to have a large region of linearly unstable but convectively stable traffic, we introduced a “resignation effect”, i.e. a density-dependent reduction of the desired velocity  $V_0$  to  $V'_0(\rho) = V_0 - \Delta V / \{ 1 + \exp[(\rho'_c - \rho)/\Delta\rho'] \}$  with  $\Delta V = 0.9V_0$ ,  $\rho'_c = 0.45\rho_{\max}$ , and  $\Delta\rho' = 0.1\rho_{\max}$ .